Pharmaceutical Sciences 2026;32(2):243-250
doi:10.34172/PS.026.42693
https://ps.tbzmed.ac.ir/

Original Article

A Laser Monitoring Technique for Investigating the Solubility and Thermodynamic Properties of Ivermectin in Aqueous Mixtures of Ethylene Glycol

Soma Khezri[1], Reza Ghotaslou[2], Kader Poturcu[3], Vahid Jouyban-Gharamaleki[4,5], Elaheh Rahimpour[1*], Abolghasem Jouyban[1]

[1]Pharmaceutical Analysis Research Center and Faculty of Pharmacy, Tabriz University of Medical Sciences, Tabriz, Iran
[2]Infectious and Tropical Diseases Research Center, Tabriz University of Medical Sciences, Tabriz, Iran
[3]Department of Chemistry, Faculty of Engineering and Natural Science, Suleyman Demirel University, Isparta, Türkiye
[4]Liver and Gastrointestinal Diseases Research Center, Tabriz University of Medical Sciences, Tabriz, Iran
[5]Kimia Idea Pardaz Azarbayjan (KIPA) Science Based Company, Tabriz University of Medical Sciences, Tabriz, Iran

ARTICLE INFO

Article History:
Received: May 20, 2025
Revised: September 10, 2025
Accepted: September 13, 2025
ePublished: April 30, 2026

Keywords:
Ivermectin, Laser monitoring technique, Mathematical modeling, Thermodynamic parameters

Abstract

Background: Ivermectin (IVM) is a broad-spectrum antiparasitic drug used in humans and animals to treat infections like scabies, river blindness, and various worms. Derived from avermectin via fermentation, IVM contains impurities and degradation products. During pandemics like COVID-19, demand for IVM formulations surges, requiring specialized manufacturing. Classified as a Biopharmaceutics Class II drug, IVM has high permeability but low solubility, leading to poor dissolution and variable absorption, impacting efficacy. Enhancing solubility can improve bioavailability and aid in purification, crystallization, and analysis. Thus, optimizing IVM formulations is crucial for better therapeutic outcomes.

Methods: This work investigated the IVM solubility in binary mixtures of ethylene glycol and water, at a temperature range of 298.2 K to 313.2 K. A laser-based robotic system was employed to measure the solubility data. The generated solubility values were presented utilizing various thermodynamic models, such as the van't Hoff, mixture response surface, Jouyban-Acree, Jouyban-Acree-van't Hoff, and modified Wilson models. Several thermodynamic factors, including $\Delta G°$, $\Delta H°$, and $\Delta S°$ were also computed according to the experimental findings.

Results: The results showed that in the EG -rich mixtures and proportional to temperature, the IVM solubility significantly increased. The mathematical models effectively estimated IVM solubility in binary solvents, with MRD% ranging from 5.7 to 13.7. Thermodynamic analysis revealed non-spontaneous dissolution, and endothermic reaction for IVM dissolution in the investigated mixtures.

Conclusion: These properties offered valuable insights into the energetic characteristics of the dissolution process and computed utilizing the Gibbs and van't Hoff equations.

Introduction

Ivermectin (IVM) possesses a wide-ranging antiparasitic effect against various internal and external nematodes and arthropods.[1] It has been- utilized generally in humans, cattle, and other animals. This medication is commonly employed to address parasitic infections such as head lice, scabies, rashes, river blindness, lymphatic filariasis, and several types of worms, including gastrointestinal roundworms, lungworms, heartworms, pinworms, and whipworms.[2] IVM is a semi-synthetic medication, derived from avermectin via a fermentation process. Avermectin is the initial material used to produce bulk IVM. During fermentation, numerous isomers are generated, which are incorporated into the bulk IVM drug substance. Consequently, typical bulk batches of IVM contain significant amounts of process-related impurities and degradation products.[3] It should be noted that during pandemic situations such as the COVID-19 outbreak, there may be a significant demand for IVM pharmaceutical formulations on a large scale. So, preparing and purifying these bulk solid oral dosage forms, including tablets and capsules, requires specialized manufacturing infrastructure and considerable resources. Additionally, IVM is classified as a class II drug under the Biopharmaceutics Classification System, characterized by high permeability but poor water solubility (0.005 mg/mL). Due to these characteristics, the drug dissolves poorly, resulting in inconsistent absorption that may

***Corresponding Author:** Elaheh Rahimpour, Email: rahimpour_e@yahoo.com

reduce its bioavailability and therapeutic effectiveness.[4] Improving drug solubility enhances oral bioavailability and is also beneficial for purification, crystallization, separation, and analytical processes.[5] Different methods have been developed to solve the problem of poor solubility. The methods involve cosolvency, solid dispersion, particle size minimization, crystal engineering, salt formation, surfactant addition, complexation, pH tuning, nanosuspension, chemical modification, and hydrotropy.[6] Cosolvency represents a frequently utilized strategy among these solubility-enhancing techniques.[7] Cosolvency studies contribute valuable knowledge about mixed solvent-solute interactions, opening doors for multidisciplinary applications.

So far, limited data have been published for the IVM solubility, which includes some monosolvents such as water, N-methyl-2-pyrrolidone, 2-pyrrolidone, triacetin, and benzyl benzoate,[8] as well as various oils including cod liver oil, castor oil, isopropyl myristate, triacetin, rose oil, isopropyl palmitate, soybean oil, olive oil, almond oil, coconut oil, in addition to surfactants like Tween 20, 60, and 80, and co-surfactants such as Span 20, 80, and polyethylene glycol 400.[9] The binary systems reported for IVM were ethanol/methanol + water mixtures published by Xu et al[10] and 1-propanol/2-propanol + water mixtures by Khezri et al.[11] However, detailed information about its solubility in additional binary solvent mixtures is still limited.

Herein, an automated laser-based technique was utilized to measure IVM solubility. The experimental procedure involves employing a mechanical arm to add the drug powder to the solubility vessel while monitoring the particles within the vessel using a laser beam. To date, our team has applied this system to explore and report the solubility of different drugs in binary mixtures. The objectives of the current work were to (1) measure the IVM solubility in aqueous mixtures of ethylene glycol (EG); (2) fit the data to several mathematical models; and (3) analyze the thermodynamic properties of IVM dissolution in the studied mixtures.

Materials and Methods

Materials

Herein, IVM served as the solute, while EG and distilled water were used to prepare the solvent mixtures. Table 1 summarizes their chemical structures, purity levels, and sources.

X-ray powder diffraction (XRD) and differential scanning calorimeter (DSC) analysis

Crystallinity analysis of IVM in various states (raw, residual powder after equilibrated in neat EG/water) was carried out via XRD (Philips PW1730). The diffraction patterns were recorded from 10° to 40° 2θ using 30 mA current and 40 kV voltage under normal atmospheric conditions. For the analysis, initially an excess of the drug powder was added to the solvents being examined, allowing them to reach equilibrium under experimental conditions. After equilibrium is established, the supernatant solution was separated and the residual solid in the container was dried for analysis. It is noteworthy that, due to the high boiling point of the non-volatile solvent EG, the residual solid was washed several times with ethanol, and eventually, XRD is performed on the final dried product, as described in a previously published article.[12]

A TA Instruments SDT 650 Simultaneous DSC/TGA (New Castle, USA) was also utilized to study the melting point of raw IVM and residual powder after equilibrated in neat EG/water. The DSC conditions were: scanning rate of 10.0°C/min under O_2 (252.5 mL/min) and N_2 (250.0 mL/min) gaseous.

Solubility determination

The solubility of IVM in EG and water mixtures was determined using a laboratory-designed setup at temperatures ranging from 298.2 to 313.2 K under ambient pressure conditions (≈85 kPa). The operational principles of this apparatus have been explained completely in our earlier publication.[13] In this approach, saturation is achieved by progressively introducing solid drug material into an initially unsaturated solvent mixture. The instrument uses laser monitoring to track changes in the drug particles as they dissolve in the solution. The solubility data were obtained by quantifying the drug

Table 1. Details of the chemical structure and purity of the used materials[a]

Material	Molecular formula	Molar mass (g mol^{-1})	Molecular structure	Mass fraction purity	Source
IVM	$C_{48}H_{74}O_{14}$	875.106	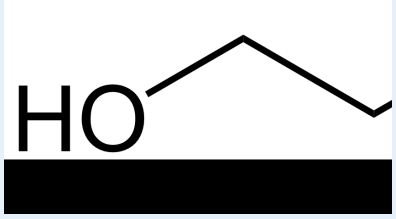	>0.999	Bekir Karliga Deva Holding (Turkey)
EG	$C_2H_6O_2$	62.068	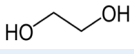	0.998	Sigma Aldrich (USA)
Water	H_2O	18.02	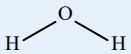	Distilled deionized water	Lab made

[a] The purity of the employed chemicals was provided by the suppliers.

mass added to the dissolution medium using gravimetric analysis. In the robotic setup, the entire processing time is reduced to just 10 to 15 minutes, which includes preparing the solvent and weighing the powder at both the beginning and end of the test. A laser beam with a wavelength between 650 and 750 nm is utilized to detect changes in the drug particles. The volumes of solvent used in this technique range from a minimum of 100 mL to a maximum of 320 mL. The mixing occurs in a closed environment to minimize evaporation and facilitate the solubility assessment in various solvents, whether binary, multiple, aquatic, or non-aquatic. For conducting an experiment with this system, the process starts with adjusting the temperature before the solute powder is added to the dissolution vessel using a robotic arm, which can accommodate either mono- or mixed solvents. During laser monitoring, a magnetic stirrer homogenizes the solution in the dissolution vessel. An automated robot incrementally introduces solute powder until the initially undersaturated solution achieves saturation, signaled by a green indicator light. The system verifies the saturation point at programmed intervals. To calculate solubility, the dispensed powder mass is gravimetrically determined post-addition.[14]

Mole fraction solubility for IVM was obtained using equation (1).

$$x = \frac{m_1 / M_1}{m_1 / M_1 + m_2 / M_2} \quad (1)$$

where m_1 and m_2 are the mass (g) of the dispended solute and solvent, respectively and M_1 and M_2 are the molar mass (g.mol^{-1}) of solute and solvent, respectively. The reported values were the mean of three replicated measurements.

Mathematical computations

Herein, some well-known models were used to investigate the correlation between solubility data, temperature, and solvent compositions. The equations checked include the van't Hoff, Jouyban-Acree, Jouyban-Acree-van't Hoff, mixture response surface (MRS), and modified Wilson models. The van't Hoff equation (Equation 2[15]) demonstrates the relationship between temperature and solute dissolution in solvent mixtures. The MRS model (Equation 3[16]) establishes the relationship between solvent composition and drug solubility at a specified temperature. The Jouyban-Acree model (Equation 4) and the Jouyban-Acree-van't Hoff model (Equation 5[17]) establish quantitative solubility relationships incorporating both compositional and thermal variables. Finally, the modified Wilson model (Equation 6[18]), as a non-linear equation, establishes the composition-solubility relationship at a specified temperature.

$$\ln x = A + \frac{B}{T} \quad (2)$$

$$\ln x_m = \beta_1 w_1' + \beta_2 w_2' + \beta_3 \left(\frac{1}{w_1'}\right) + \beta_4 \left(\frac{1}{w_2'}\right) + \beta_5 w_1'.\, w_2' \quad (3)$$

$$\ln x_{m,T} = w_1 \ln x_{1,T} + w_2 \ln x_{2,T} + \frac{w_1.w_2}{T} \sum_{i=0}^{2} J_i.\left(w_1 - w_2\right)^i \quad (4)$$

$$\ln x_{m,T} = w_1\left(A_1 + \frac{B_1}{T}\right) + w_2\left(A_2 + \frac{B_2}{T}\right) + \frac{w_1.w_2}{T} \sum_{i=0}^{2} J_i.\left(w_1 - w_2\right)^i \quad (5)$$

$$-\ln x_m = 1 - \frac{w_1\left[1 + \ln x_1\right]}{w_1 + w_2\lambda_{12}} - \frac{w_2\left[1 + \ln x_2\right]}{w_1\lambda_{21} + w_2} \quad (6)$$

In which, the solubilities of the solute in the solvent mixtures and mono-solvents 1 and 2 are represented by x_m, x_1 and x_2, respectively, while the mass fractions of solvent 1 and solvent 2 are w_1 and w_2. Other parameters *A*, *B*, *Ji*, *βi*, λ_{ij} are model parameters and were obtained from linear and non-linear regressions. The mean relative deviation (*MRD* %) (Equation 7) is used to express the model accuracy.

$$MRD\% = \frac{100}{N} \Sigma \left(\frac{\left| Calculated\ Value - Observed\ Value \right|}{Observed\ Value} \right) \quad (7)$$

The *N* is the data point number.

Computation of appearance thermodynamic parameters

Thermodynamic analysis was performed using the van't Hoff equation to determine key parameters, including the standard dissolution enthalpy (*ΔH°*), Gibbs free energy change (*ΔG°*), and standard dissolution entropy (*ΔS°*) of IVM in EG-water mixtures.[19] The van't Hoff equation was employed to calculate the *ΔH°* in these solvent mixtures, as follows:

$$\frac{\partial \ln x}{\partial\left(\frac{1}{T} - \frac{1}{T_{hm}}\right)_p} = -\frac{\Delta H^\circ}{R} \quad (8)$$

Here, *R* is the ideal gas constant and T_{hm} represents the mean harmonic temperature acquired by $T_{hm} = n / \sum_{i=1}^{n}(1/T)$, where *n* is the number of the tested temperatures. Herein, T_{hm} value is 305.6 K. The *ΔH°* value is obtained by plotting ln*x* against (1/T - 1/T_{hm}) (Equation 8). The plot slope is utilized to compute *ΔH°*. We assume constant solution heat capacity change between 298.2 and 313.2 K. The *ΔG°* and *ΔH°* values are also, computed from the intercept and slope of the plot in Equation 8, respectively. The Gibbs equation is then used to compute *ΔS°* using *ΔH°* and *ΔG°* (Equation 9):

$$\Delta S^\circ = \frac{\Delta H^\circ - \Delta G^\circ}{T_{hm}} \quad (9)$$

As both enthalpy and entropy have key roles in the dissolution process, their contributions (ζ_{TS} and ζ_H) can be obtained using Equations 10 and 11:

$$\zeta_{TS} = \frac{\left|T\Delta S^\circ\right|}{\left(\left|\Delta H^\circ\right| + \left|T\Delta S^\circ\right|\right)} \quad (10)$$

$$\zeta_H = \frac{|\Delta H^\circ|}{\left(|\Delta H^\circ| + |T\Delta S^\circ|\right)} \quad (11)$$

Results and Discussion

XRD and DSC analysis

Figure 1 showed the XRD data for IVM residues in the investigated solvents of EG and water. This analysis aimed to identify whether solid IVM in saturated solutions produced solvated or polymorphic compounds. The results indicated that no new characteristic peaks appeared, implying that the crystallinity of IVM (as reported in reference[20]) remained stable and did not experience polymorphic transformation during dissolution in the solvents examined.

DSC analysis was used to determine the melting points of both raw and equilibrated IVM in the used solvents. As can be seen in Figure 2, the melting point of raw IVM (153.8 ± 0.5 °C,[4]), derived from the peak temperature in the DSC curves, was similar for both forms (*i.e.,* residual in EG with melting point 155.3 ± 0.5 °C and residual in water with melting point 154.3 ± 0.5 °C), indicating that the crystallinity of raw IVM remained unchanged after dissolution procedure in the studied solvents.

Solubility profile of ivermectin

IVM's solubility in mixtures of EG + water can be understood through the analysis of the data presented in Table 2. The Table displayed temperature-dependent solubility measurements (expressed as mole fractions) at different EG compositions, with associated standard deviations. ideal solubility calculations for the 298.2-313.2 K range are also included. The ideal solubility was calculated using literature-reported values of IVM's melting temperature (T_M) and enthalpy of fusion (ΔH_f). (T_M = 430.15 K[21], ΔH_f = 61 KJ/mol). For better visual comprehension, the solubility profile of IVM was also plotted in Figure 3. In this solubility system, the lowest solubility of IVM was obtained in neat water at 298.2 K ($x_m = 4.97 \times 10^{-6}$) and the highest solubility was reported when the mixtures contained the highest concentrations of EG ($w_1 = 1.0$, neat EG). Moreover, the solubility of IVM increased with rising temperature. Considering that IVM with log P = 5.83[9], dipole moment: 4.14 D[22] and Hansen solubility parameters of $\delta_D = 18.0$, $\delta_P = 12.80$, $\delta_H = 10.01$ (Hansen solubility parameters were obtained from Hoy software[23]), EG with log P = -1.69, dipole moment: 2.27 D, dielectric constant of 37.0 and Hansen solubility parameters of $\delta_D = 17.0$, $\delta_P = 11.0$, $\delta_H = 26.0$, and water with dipole moment: 1.85 D,[24] a dielectric constant of 78.4[25] and Hansen solubility parameters of $\delta_D = 15.50$, $\delta_P = 16.00$, $\delta_H = 42.30$, the solubility of IVM in EG was expected to be higher than in water owing to the similarity in their molecular structures, as indicated by their Hansen solubility parameters.

The solubility of IVM in water at 298.2 K ($x_m = 4.97 \times 10^{-6}$) measured in this study was compared with the literature data which were 5.60×10^{-6},[11] demonstrating the close agreement and validity of the results from this study.

Solubility data modeling

The solubility data of IVM in EG + water mixtures were correlated using five thermodynamic models: van't Hoff, Jouyban-Acree, Jouyban-Acree-van't Hoff, MRS, and modified Wilson, with the fitting results summarized

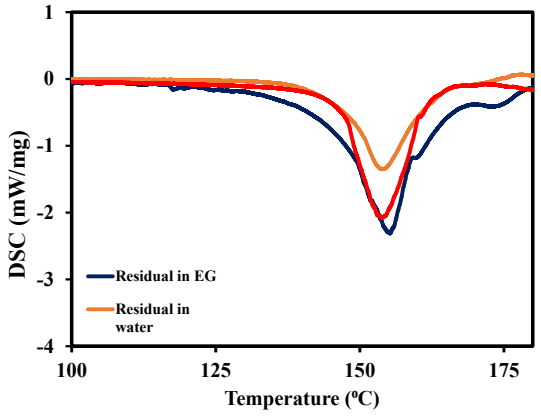

Figure 2. DSC curves of IVM in raw and equilibrated forms

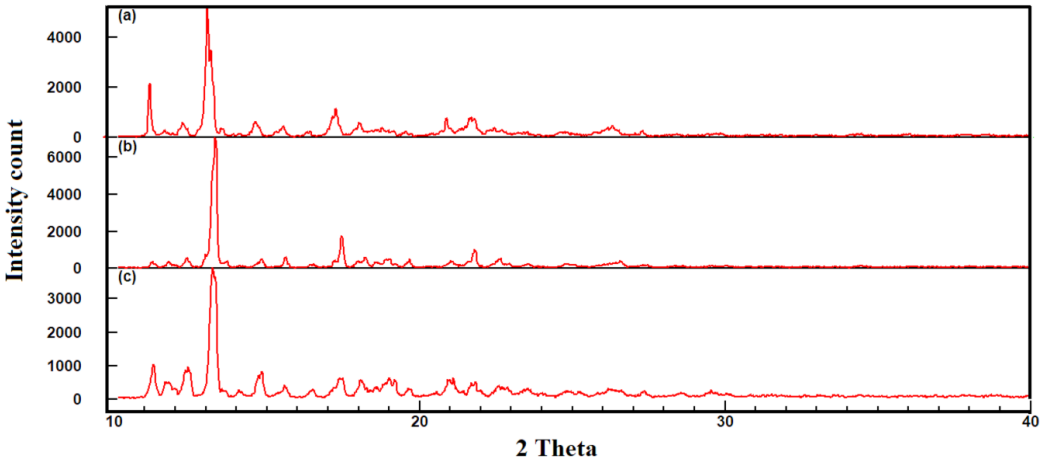

Fig. 1. XRD pattern of raw IVM (a) and equilibrated IVM in EG (b), and water (c)

Table 2. Experimental mole fraction solubility ($x_{m,T}$) values (±SD) for IVM in EG + water mixtures at different temperatures and ambient pressure (≈ 85 kPa)

w_1 [a]	298.2 K	303.2 K	308.2 K	313.2 K
0.00	$4.97\ (\pm0.09)\times10^{-6}$	$9.94\ (\pm0.11)\times10^{-6}$	$1.37\ (\pm0.08)\times10^{-5}$	$1.71\ (\pm0.14)\times10^{-5}$
0.10	$7.56(\pm0.10)\times10^{-6}$	$1.57\ (\pm0.12)\times10^{-5}$	$2.10\ (\pm0.11)\times10^{-5}$	$2.77\ (\pm0.09)\times10^{-5}$
0.30	$8.49\ (\pm0.08)\times10^{-6}$	$1.61\ (\pm0.09)\times10^{-5}$	$2.28\ (\pm0.10)\times10^{-5}$	$2.81\ (\pm0.11)\times10^{-5}$
0.50	$1.67\ (\pm0.09)\times10^{-5}$	$2.31\ (\pm0.09)\times10^{-5}$	$3.34\ (\pm0.12)\times10^{-5}$	$4.28\ (\pm0.09)\times10^{-5}$
0.70	$2.39\ (\pm0.11)\times10^{-5}$	$3.13\ (\pm0.09)\times10^{-5}$	$4.62\ (\pm0.10)\times10^{-5}$	$5.59\ (\pm0.08)\times10^{-5}$
0.90	$8.40\ (\pm0.13)\times10^{-5}$	$9.52\ (\pm0.11)\times10^{-5}$	$1.15\ (\pm0.09)\times10^{-4}$	$1.19\ (\pm0.11)\times10^{-4}$
1.00	$2.67\ (\pm0.10)\times10^{-4}$	$2.86\ (\pm0.08)\times10^{-4}$	$2.99\ (\pm0.11)\times10^{-4}$	$3.14\ (\pm0.11)\times10^{-4}$
Ideal x	5.28×10^{-4}	7.92×10^{-4}	1.17×10^{-3}	1.71×10^{-3}

[a] w_1 is the mass fraction of EG in EG and water mixtures in the absence of ivermectin.
Standard uncertainty u is u(T) = ±0.1K; u(p) = ±0.05 bar. Also, relative standard uncertainties are obtained below 5% for mole fractions and solubilities. The value of the coverage factor k = 2 was chosen based on the level of confidence of approximately 95%.

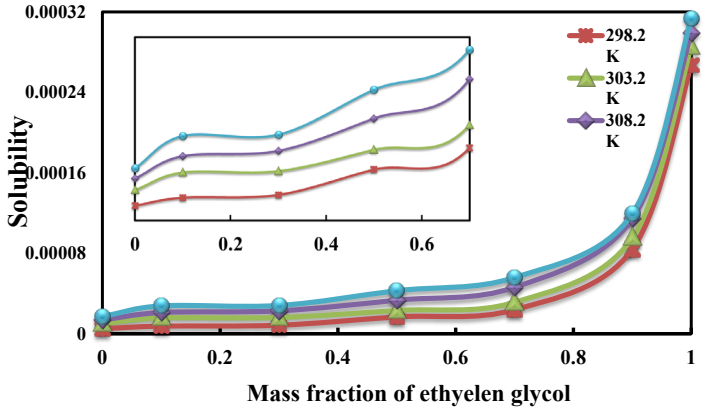

Figure 3. Solubility profile of for IVM in EG + water mixtures at 298.2-313.2 K

in Tables 3-6. The models were evaluated based on their *MRD*% between the calculated and measured data. In Table 3, the van't Hoff model showed overall *MRD*% values of 5.7% indicate that the van't Hoff model successfully predicted the solubility of IVM in this system. Additionally, the parameters *A* and *B* for the van't Hoff model were also listed in Table 3. Table 4 summarizes the parameters for both Jouyban-Acree-based models, with calculated *MRD*% values of 9.1% (Jouyban-Acree) and 11.4% (Jouyban-Acree-van't Hoff) for the system. Table 5 also detailed the constants of the MRS model for different temperatures and provided the *MRD*% values for the solubility of IVM in EG + water mixtures. The *MRD*% value for the back-calculated solubility data was 13.7% suggesting that the MRS model demonstrates acceptable predictive accuracy in this system. Table 6 displays the temperature-dependent parameters of the modified Wilson model and their associated *MRD*% values. The overall *MRD*% value for the back-calculated IVM solubility data was 12.1% indicating relatively good predictive performance for this system. Notably, all models showed similar predictive capability, as evidenced by the small variations in their *MRD*% values.

To further investigate the predictive capability of the Jouyban-Acree-van't Hoff model, a training method was employed with a minimal set of data points. The pure solvent data (all temperatures) and selected mixture data (0.3, 0.5, and 0.7 mass fractions at 298.2 K) were used for model training, and the it was used for solubility prediction across untested conditions. The prediction *MRD*% values obtained were 10.9%, 17.6%, 17.3%, and 13.8% at various temperatures, respectively.

Table 7 presented the Napierian logarithmic activity constants of IVM in EG-water binary mixtures, as determined by the NRTL model.[26] The findings indicated that IVM solubility increases when its activity coefficient decreases, which is attributed to stronger interactions between IVM molecules and the EG-rich mixture.[27] This relationship was further illustrated in Figure 4.

Hansen solubility parameter

Choosing suitable solvents serves as the foundation for effective solvent replacement. The Hansen Solubility Parameters (HSP) method provides a simple and efficient way to predict and choose suitable solvent mixtures based on solubility data. Hildebrand and Scott proposed the solubility parameter (δ) concept, establishing that components with comparable δ values demonstrate greater miscibility and enhanced solubility.[28] Hansen's theory establishes that a component's solubility parameter (δ) comprises three contributions: hydrogen bonding, polar interactions, and dispersion forces.[29] The total solubility parameter (Hildebrand, δ_t) represents the square root of the sum of the squares of the three HSP

Table 3. The van't Hoff model constants and the *MRD*% for backcalculated data for IVM in EG + water mixtures

w_1	van't Hoff model		
	A	*B*	*MRD*%
0.00	13.279	-7564.967	11.1
0.10	14.636	-7843.301	10.6
0.30	13.157	-7373.193	10.1
0.50	8.946	-5945.573	1.85
0.70	7.806	-5501.914	3.1
0.90	-1.618	-2313.366	2.5
1.00	-4.898	-991.615	0.4
Overall MRD%			5.7

Table 4. The Jouyban-Acree, and Jouyban-Acree-van't Hoff model constants and the *MRD*% for backcalculated data for IVM in EG + water mixtures

Jouyban-Acree		Jouyban-Acree-van't Hoff	
J_0	-1018.593	A_1	-4.898
J_1	-1329.061	B_1	-991.615
J_2	0[a]	A_2	13.279
		B_2	-7564.967
		J_0	-1018.094
		J_1	-1328.704
		J_2	0[a]
MRD%	9.1		11.4

[a] Not statistically significant (*P* value > 0.05).

Table 5. The MRS model constants and the *MRD*% for backcalculated data for IVM in EG + water mixtures

T (K)	β_1	β_2	β_3	β_4	β_5	*MRD*%
298.2	-9.657	-12.338	0[a]	0.030	0[a]	16.0
303.2	-9.624	-11.565	0[a]	0.031	0[a]	15.9
308.2	-9.293	-11.225	0[a]	0.025	0[a]	12.1
313.2	-9.189	-10.950	0[a]	0.023	0[a]	10.7
Overall MRD%						13.7

[a] Not statistically significant (*P* value > 0.05)

Table 6. The modified Wilson model constants and the *MRD*% for backcalculated data for IVM in EG + water mixtures

T (K)	modified Wilson model		
	λ_{12}	λ_{21}	*MRD*%
298.2	3.106	0.322	11.5
303.2	3.850	0.260	11.5
308.2	3.171	0.315	11.6
313.2	3.042	0.329	13.8
Overall MRD%			12.1

Table 7. The calculated ln (γ) of IVM in the aqueous mixtures of EG based on NRTL model at *T* = (298.2–313.2) K

w_1	ln (γ)			
	298.2 K	303.2 K	308.2 K	313.2 K
0.00	4.665	4.378	4.449	4.608
0.10	4.246	3.921	4.022	4.125
0.30	4.13	3.895	3.94	4.111
0.50	3.453	3.534	3.558	3.69
0.70	3.095	3.231	3.234	3.423
0.90	1.838	2.118	2.322	2.668
1.00	0.681	1.018	1.366	1.697

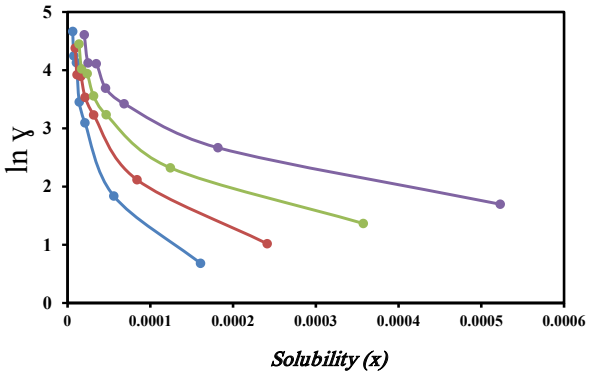

Figure 4. The relationship of calculated solubility *x* (IVM) with NRTL model and activity coefficient (γ) for IVM in the aqueous mixtures of EG from NRTL model at investigated temperature

components. Comparing these parameters helps quantify solvent-solute compatibility. The following mathematical relationship was proposed by Hansen to calculate the HSP difference between solvent and solute components:

$$\Delta\delta_{i,j} = \sqrt{4\left(\delta_d^i - \delta_d^j\right)^2 + \left(\delta_p^i - \delta_p^j\right)^2 + \left(\delta_h^i - \delta_h^j\right)^2} \quad (12)$$

where $\Delta\delta_{i,j}$ denotes to the dissimilarity factor, and the *j* and *i* superscripts relates to the solute and the solvent, respectively. Table 8 presents the obtained δ_d (dispersion), δ_p (polar), and δ_h (hydrogen bonding) parameters for IVM, EG, and water. The data indicate that the δ_d and δ_p of IVM play a significant role in its solubility behavior due to the similarity in parameters with EG. Notably, the lower $\Delta\delta$ values observed for IVM in EG compared to water indicate stronger compatibility, explaining why IVM demonstrates greater solubility in EG-water mixtures than in neat aqueous solutions. This behavior aligns with HSP theory, where smaller $\Delta\delta$ values correlate with improved miscibility.

Computation of apparent thermodynamic properties

Table 9 presented the apparent thermodynamic factors of the IVM dissolution in EG + water system at 305.6 K. The factors included $\Delta G°$, $\Delta H°$, $\Delta S°$, $T\Delta S°$, ζ_H, and ζ_{TS}. The thermodynamic analysis showed favorable dissolution of IVM in these mixtures, though positive ΔG° values demonstrated the process was non-spontaneous at saturation, while the positive $\Delta H°$ values showed an endothermic reaction, indicating that heat was absorbed during the dissolution. Moreover, the positive $\Delta S°$ values (except for EG mass fractions of 0.9 and 1.0) suggested that entropy played a beneficial role in the dissolution process. Moreover, as evidenced by ζ_H being greater than

Table 8. The HSP for the materials

Name	δ_d (MPa$^{1/2}$)	δ_p (MPa$^{1/2}$)	δ_h (MPa$^{1/2}$)	δ_t (MPa$^{1/2}$)
Water	15.5	16.0	42.3	47.8
EG	17.0	11.0	26.0	32.95
IVM	18.09	12.72	9.59	24.11
$\Delta\delta_{ij}$				
Solute			**Co-solvent**	
IVM		EG		water
		16.64		33.27

Table 9. Apparent thermodynamic parameters of IVM dissolution in EG + water mixtures at T_{hm} = 305.6 K and ambient pressure (≈ 85 kPa)

w_1	$\Delta G°$ (kJ.mol^{-1})	$\Delta H°$ (kJ.mol^{-1})	$\Delta S°$ (J.K^{-1}.mol^{-1})	$T\Delta S°$ (kJ.mol^{-1})	ζ_H	ζ_{TS}
0.00	29.16	62.90	110.41	33.74	0.651	0.349
0.10	28.02	65.21	121.68	37.18	0.637	0.363
0.30	27.87	61.30	109.39	33.43	0.647	0.353
0.50	26.70	49.43	74.37	22.73	0.685	0.315
0.70	25.91	45.74	64.90	19.83	0.698	0.302
0.90	23.34	19.23	-13.45	-4.11	0.824	0.176
1.00	20.69	8.24	-40.72	-12.44	0.399	0.601

ζ_{TS} (except for neat EG), the enthalpy contribution played a dominant role in these mixtures. This showed that a significant amount of energy was needed to overcome the interactions between the drug, solvent, and co-solvent. In summary, IVM dissolution in EG-water mixtures was thermodynamically favorable, primarily governed by decreasing $\Delta G°$ and endothermic behavior.

Enthalpy–entropy compensation analysis

Figure 5 presented the enthalpy-entropy compensation plot, which showed the relationship between $\Delta H°$ and $\Delta G°$ regarding the solubility of IVM in EG + water mixtures at T_{hm}. The plot elucidated the respective contributions of $\Delta S°$ and enthalpy $\Delta H°$ changes to the dissolution thermodynamics. In Figure 5, the negative slope observed for mass fractions ranging from 0.0 to 0.1 indicates that the solubility enhancement of IVM in this range was primarily driven by entropic effects. This suggests that at low co-solvent concentrations, the increase in solubility arose from greater molecular disorder or improved solvent mixing, rather than strong energetic interactions. In contrast, the positive slope seen at higher mass fractions (0.1–1.0) implies that solubility enhancement in this region was more influenced by enthalpic contributions, where favorable solute-solvent interactions, such as hydrogen bonding or van der Waals forces, played a dominant role. The study revealed enthalpy-entropy compensation behavior, with progressive $\Delta H°$ enhancement during dissolution being compensated by commensurate $\Delta S°$ elevation, manifesting as a linear $\Delta H°$-$\Delta S°$ relationship. This compensation effect demonstrated that both entropy and enthalpy were key factors governing IVM dissolution, with entropic effects prevailing at low co-solvent fractions

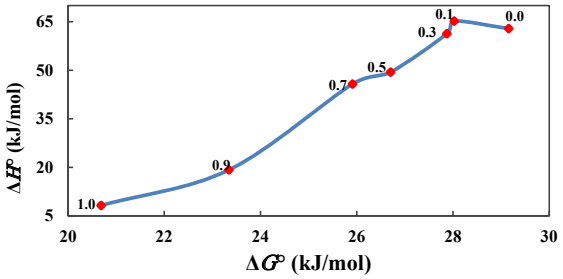

Figure 5. Enthalpy-entropy compensation plot for the IVM solubility in EG + water mixtures at T_{hm} = 305.6 K. The solid data points represent the EG mass fractions in the binary solvent mixtures prior to IVM addition

and enthalpic effects becoming more significant at higher concentrations. The interplay between these thermodynamic parameters ensured a balanced solubility profile across the entire solvent composition range.

Conclusion

This work investigated the temperature-dependent solubility and dissolution thermodynamics of IVM in binary EG + water solvent systems. The results showed that in the EG -rich mixtures and proportional to temperature, the IVM solubility significantly increased. While manual experimental methods yield reliable solubility data, they present several limitations including impracticality, labor-intensive procedures, time consumption, and high costs. A promising approach involves employing mathematical predictive models to estimate solubility, enabling interpolation between experimental data points and identification of potential outliers. Some of well-known methods were employed herein to correlate and back-calculate the IVM solubility data. These models effectively predicted IVM solubility in the binary solvent mixtures, achieving an *MRD*% of 5.7 for the van't Hoff, 9.1 for the Jouyban-Acree, 11.4 for the Jouyban-Acree-van't Hoff, 13.7 for the MRS, and 12.1 for the modified Wilson models concluding that these models served as effective tools for predicting solubility in alternative solvent systems and determining key thermodynamic properties. Moreover, in the thermodynamic analysis, positive $\Delta G°$ values indicating a non-spontaneous manner of dissolution process, the positive $\Delta H°$ values showing an endothermic reaction, and the positive $\Delta S°$ values (except for EG mass fractions of 0.9 and 1.0) suggesting the beneficial role of the entropy in the dissolution process.

Authors' Contribution

Conceptualization: Abolghasem Jouyban, Elaheh Rahimpour.
Data curation: Soma Khezri, Kader Poturcu.
Funding acquisition: Reza Ghotaslou.
Investigation: Soma Khezri, Kader Poturcu.
Methodology: Elaheh Rahimpour.
Project administration: Elaheh Rahimpour.
Resources: Reza Ghotaslou.
Software: Vahid Jouyban-Gharamaleki.
Supervision: Elaheh Rahimpour, Abolghasem Jouyban.
Validation: Vahid Jouyban-Gharamaleki.
Visualization: Reza Ghotaslou.

Writing–original draft: Elaheh Rahimpour.
Writing–review & editing: Reza Ghotaslou, Abolghasem Jouyban.

Competing Interests
The authors declare that they have no competing interests.

Consent for Publication
Not applicable

Data Availability Statement
The datasets used and/or analysed during the current study are available from the corresponding author on reasonable request.

Ethical Approval
Not applicable.

Funding
Research reported in this publication was supported by Elite Researcher Grant Committee under grant number 4003663 from the National Institutes for Medical Research Development (NIMAD), Tehran, Iran.

References
1. Crump A, Ōmura S. Ivermectin, 'wonder drug' from Japan: the human use perspective. Proc Jpn Acad Ser B Phys Biol Sci. 2011;87(2):13-28. doi: 10.2183/pjab.87.13
2. Daurio CP, Cheung EN, Jeffcoat AR, Skelly BJ. Bioavailability of ivermectin administered orally to dogs. Vet Res Commun. 1992;16(2):125-30. doi: 10.1007/bf01839009
3. Fink DW, Porras AG. Pharmacokinetics of ivermectin in animals and humans. In: Campbell WC, ed. Ivermectin and Abamectin. New York: Springer; 1989. p. 113-30. doi: 10.1007/978-1-4612-3626-9_7
4. Yılmaz M, Toprak C, Gün G, Özbek M. Development of bulk homogenity with formulation of ivermectin tablet by geometric blending. Res Rev J Pharm Pharm Sci. 2021;10(2):1-8.
5. Mohammadian E, Barzegar-Jalali M, Rahimpour E. Solubility prediction of lamotrigine in cosolvency systems using Abraham and Hansen solvation parameters. J Mol Liq. 2019;276:675-9. doi: 10.1016/j.molliq.2018.12.043
6. Sareen S, Mathew G, Joseph L. Improvement in solubility of poor water-soluble drugs by solid dispersion. Int J Pharm Investig. 2012;2(1):12-7. doi: 10.4103/2230-973x.96921
7. Jouyban A. Review of the cosolvency models for predicting solubility in solvent mixtures: an update. J Pharm Pharm Sci. 2019;22(1):466-85. doi: 10.18433/jpps30611
8. Camargo JA, Sapin A, Nouvel C, Daloz D, Leonard M, Bonneaux F, et al. Injectable PLA-based in situ forming implants for controlled release of Ivermectin a BCS Class II drug: solvent selection based on physico-chemical characterization. Drug Dev Ind Pharm. 2013;39(1):146-55. doi: 10.3109/03639045.2012.660952
9. Patel VP, Lakkad HA, Ashara KC. Formulation studies of solid self-emulsifying drug delivery system of ivermectin. Folia Med (Plovdiv). 2018;60(4):580-93. doi: 10.2478/folmed-2018-0024
10. Xu H, Jiang L, Wang L. Determination and correlation of solubilities of ivermectin in alcohol and alcohol-water mixture. J Nanjing Univ Sci Technol. 2014;38:173-80.
11. Khezri S, Ghotaslou R, Poturcu K, Soleymani J, Rahimpour E, Jouyban A. Solubility and thermodynamics of ivermectin in aqueous mixtures of 1-propanol/2-propanol. J Solution Chem. 2025;54(1):92-108. doi: 10.1007/s10953-024-01416-1
12. Rahimpour E, Jouyban A. A simple strategy for washing a recrystallized drug from viscous and non-volatile solvents prior to XRD study: a technical note. Rev Colomb Cienc Quim Farm. 2023;52(1):107-13. doi: 10.15446/rcciquifa.v52n1.109364
13. Jouyban-Gharamaleki V, Jouyban A, Kuentz M, Hemmati S, Martinez F, Rahimpour E. A laser monitoring technique for determination of mesalazine solubility in propylene glycol and ethanol mixtures at various temperatures. J Mol Liq. 2020;304:112714. doi: 10.1016/j.molliq.2020.112714
14. Zarghampour A, Jouyban K, Jouyban-Gharamaleki V, Jouyban A, Rahimpour E. A description on the shake-flask and laser monitoring-based techniques for determination of the drug's solubility. Pharm Sci. 2024;30(2):274-8. doi: 10.34172/ps.2024.2
15. Grant DJ, Mehdizadeh M, Chow AH, Fairbrother JE. Non-linear van't Hoff solubility-temperature plots and their pharmaceutical interpretation. Int J Pharm. 1984;18(1-2):25-38. doi: 10.1016/0378-5173(84)90104-2
16. Ochsner AB, Belloto RJ, Jr., Sokoloski TD. Prediction of xanthine solubilities using statistical techniques. J Pharm Sci. 1985;74(2):132-5. doi: 10.1002/jps.2600740206
17. Jouyban A, Acree WE Jr. Mathematical derivation of the Jouyban-Acree model to represent solute solubility data in mixed solvents at various temperatures. J Mol Liq. 2018;256:541-7. doi: 10.1016/j.molliq.2018.01.171
18. Jouyban-Gharamaleki A. The modified Wilson model and predicting drug solubility in water-cosolvent mixtures. Chem Pharm Bull. 1998;46(6):1058-61. doi: 10.1248/cpb.46.1058
19. Perlovich GL, Kurkov SV, Bauer-Brandl A. Thermodynamics of solutions. II. Flurbiprofen and diflunisal as models for studying solvation of drug substances. Eur J Pharm Sci. 2003;19(5):423-32. doi: 10.1016/s0928-0987(03)00145-3
20. Lu M, Xiong D, Sun W, Yu T, Hu Z, Ding J, et al. Sustained release ivermectin-loaded solid lipid dispersion for subcutaneous delivery: in vitro and in vivo evaluation. Drug Deliv. 2017;24(1):622-31. doi: 10.1080/10717544.2017.1284945
21. Li WL, Zhou CR, Zhang L. Investigation on specific heat capacity and combustion enthalpy of ivermectin. J Therm Anal Calorim. 2016;124(1):447-53. doi: 10.1007/s10973-015-5111-1
22. Rana M, Yadav P, Lakhera S, Chowdhury P. Ivermectin and doxycycline combination as a promising anti-viral drug candidate: an in-silico and DFT study. 2023. Res Sq [Preprint]. January 16, 2023Available from: https://www.researchsquare.com/article/rs-2471515/v1.
23. Aerts J. The Hoy Solubility Parameter Calculation Software. Germany: Computer Chemistry Counsultancy; 2005.
24. Zhu T, Van Voorhis T. Understanding the dipole moment of liquid water from a self-attractive Hartree decomposition. J Phys Chem Lett. 2021;12(1):6-12. doi: 10.1021/acs.jpclett.0c03300
25. Malmberg CG, Maryott AA. Dielectric constant of water from 0 to 100 C. J Res Natl Bur Stand (1977). 1956;56(1):1-8.
26. Behboudi E, Soleymani J, Martinez F, Jouyban A. Solubility of amlodipine besylate in acetonitrile + water binary mixtures at various temperatures: determination, modelling, and thermodynamics. Phys Chem Liq. 2022;60(6):892-909. doi: 10.1080/00319104.2022.2068012
27. Kasagić-Vujanović I, Knežević D. Design of experiments in optimization and validation of hydrophilic interaction liquid chromatography method for determination of amlodipine besylate and its impurities. Acta Chromatogr. 2021;34(1):41-52. doi: 10.1080/10826076.2014.991872
28. Hildebrand JH, Robert LS. Regular solutions. Inorg Chem. 1963;2:431-2.
29. Hansen CM. The Three-Dimensional Solubility Parameter. Copenhagen: Danish Technical Press; 1967.